Int. J. Electrochem. Sci., 15 **(2020)** 6302 – 6313, doi: 10.20964/2020.07.04

International Journal of
ELECTROCHEMICAL
SCIENCE
www.electrochemsci.org

Porous nitrogen doped carbon materials as High-Active Oxygen Reduction Catalysts Derived from Biomass (Corn Stalk)

Weimin Cao[1], *Xiaofei Guo*[1], *Chaju Zeng*[1], *Chao Yang*[1], *Wei Zhou*[1], *Qiang Liu*[2,*]

[1] College of Sciences, Shanghai University, No. 99 Shangda Rd., Shanghai 200444, P. R. China
[2] School of Environmental and Chemical Engineering, Shanghai University, No. 333 Nanchen Rd., Shanghai 200444, P. R. China
[*]E-mail: qliu@shu.edu.cn

Received: 10 January 2020 / *Accepted:* 21 March 2020 / *Published:* 10 June 2020

In this study, three catalysts (BC-Zn, BC-HP and BC-Na) were prepared by pyrolyzing corn stalk biomass with $ZnCl_2$, H_3PO_4 and NaOH acting as activator. We compare and summarize the structure and electrocatalytic activity of these carbon materials for oxygen reduction reaction (ORR). A high-performance doped carbon catalyst (BC-Na) with a BET surface area of up to 1337.27 m^2 g^{-1} was prepared by using NaOH as an activating agent. For ORR in alkaline media, BC-Zn exhibited a more negative shift of -0.42 V (*vs* Hg/HgO) in contrast to BC-HP (-0.31 V) and BC-Na (-0.31 V). Even though BC-Na showed a negative ORR onset potential (E=-0.21 V) in comparison with Pt/C (E=0.09V), its current density reached up to 5.72 mA·cm^{-2}, which is much higher than Pt/C (3.25 mA·cm^{-2}). It is supposed that the excellent electrocatalytic property of BC-Na originated from the combined effect of high specific surface area and N doping. The low-cost and simple approach used in study provides a straightforward route for the preparation of ORR electrocatalysts from biomass.

Keywords: oxygen reduction reaction, catalyst, biomass, activating agent

1. INTRODUCTION

Currently, the great challenges in energy crisis and environmental pollution urge the development of green and sustainable energy systems. Fuel cells are considered to be the most promising technology for the portable energy supply devices, which can generate electric energy by electrochemical reaction between hydrogen and oxygen (or air) without combustion process. However, the kinetics of oxygen-reduction reaction (ORR) at the cathode is limited [1,2]. So far, the reported high-performance electro-catalysts almost exclusively relied on Pt-based electro-catalysts due to the superior catalytic activity and stability [3-5]. Such as it is, the drawbacks of high cost, scarcity of raw materials and poor stability of Pt-based catalysts fundamentally hamper the further development of fuel cells [6].

Therefore, the development of efficient, inexpensive, more stable and commercially available catalysts for ORR is highly desired.

Recently, the use of nitrogen-doped (N-doped) carbon nanotube [7], N-doped graphene [8,9], graphene/carbon nanotube nanocomposite [10,11], mesoporous N-doped carbon [12], and N-doped carbon nanocages [13] as metal-free electro-catalysts for ORR have been widely studied. In addition, the pyrolytic product of crab shells [14], ovalbumin [15], ginkgo [16], egg shell [17], shrimp shells [18] and even human hair [19] have also been successfully used for the electrode materials of fuel cells. Apart from these, biomass materials were also proven as the attractive precursors of ORR catalysts since they are usually rich with sulfur, nitrogen, phosphorus elementals, and sometimes heavy metals (cumulative plant). All of these elements were reported to be involved in can develop candidate ORR active sites and thus significantly increase the activity of carbon-based catalysts [20,21].

To develop high-performance ORR material, some activation steps are frequently employed in the preparation of electrode from biomass. The common activating agent includes $ZnCl_2$, KOH, NaOH, and H_3PO_4. For example, Liu et al [22] used $ZnCl_2$ as an activation reagent to synthesize nitrogen self-doped porous carbon by a facile procedure based on simple pyrolysis at controlled temperatures (600-800 °C) using water hyacinth (*Eichhornia Crassipes*) as feedstock. Zhou et al [23] used intrinsically porous biomass (soybean shells) as a carbon and nitrogen source to synthesize porous nitrogen-doped graphene *via* calcination and KOH activation. Our previous study [24] also used KOH to prepare high-active ORR catalyst by direct co-pyrolysis of biomass with activating agent. However, the reactions between KOH and biomass are too vigorous and liable to cause the fragmentation and collapse of porous structure, and therefore affect the catalytic performance of electrode materials. For this reason, some mild activation methods are essential to be developed in the pyrolysis of biomass.

In this work, we used a common agricultural bio-waste, corn straw, as carbon and nitrogen source to prepare carbon materials (biochar) with some sample methods, including one pot co-pyrolysis of biomass with activators ($ZnCl_2$, H_3PO_4, and NaOH) and part of thermal cracking carbide with high temperature annealing. The choice of activator and synthesis methods have the following advantages: 1. sustainable biomass as precursor which obtain organic and inorganic nitrogen; 2. pyrolysis process is simple and can be manipulated without template. The obtained carbon materials were further tested as catalysts for ORR. These biochars have a high specific surface area, evenly distributed pores and uniform nitrogen doping. In alkaline media, some of the biochar exhibited similar catalytic activity as compared with commercial 20% Pt/C.

2. EXPERIMENTAL MATERIALS AND METHODS

2.1 Preparation of catalysts

Corn stalk used in this experiment was collected from Chongming Island, Shanghai, China. The biomass was washed extensively by deionized water to remove impurities and air-dried for days. Before pyrolysis, raw biomass was cut into pieces, ground to powder in a mortar, screened by a 100-mesh sieve and oven-dried at 105 °C for 24 h.

$ZnCl_2$ modified biochar (marked with BC-Zn) was prepared by following steps: 6.0 g corn stalk powder and 1.0 g $ZnCl_2$ powder (AR) was thoroughly mixed and placed into a tube furnace and heated at a rate of 10 °C·min^{-1} to 700 °C for 2 h under N_2 flow (100 mL·min^{-1}). After cooling to room temperature under N_2 gas, the carbonized product was alternately rinsed with 0.5 M HNO_3 and 1 M HCl to remove metal deposits. The product was further washed with deionized water to stable pH and dried in an oven at 80 °C. Phosphoric acid modified biochar (BC-HP) was prepared by following steps: 5.0 g biomass of corn stalk was dispersed in 20 mL phosphoric acid (85%). After 12 h, the solution was filtered and the recovered solid was oven-dried at 80 °C for 4 h. The biomass was subsequently placed into a tube furnace and heated at 850 °C under N_2 flow (100 mL·min^{-1}) for 30 min at a heating rate of 5 °C·min^{-1}. After pyrolysis, the furnace was cooled down to room temperature under N_2 gas, and the carbonized product was withdrawn and rinsed with 0.5 M $NH_3 \cdot H_2O$ and deionized water until stable pH. The rinsed sample was further dried in an oven at 90 °C for 12 h. NaOH modified biochar (marked with BC-Na) was prepared by following steps: 10.0 g biomass was first placed into a tube furnace and heated at 250 °C under N_2 flow (100 mL·min^{-1}) for 2 h. Afterward, the roasted solid was mixed with NaOH powder (AR) at a mass ratio of 1:3, and the mixture was heated at 600 °C under N_2 flow (100 mL·min^{-1}) for 1 h at a heating rate of 10 °C·min^{-1}. After pyrolysis, the furnace was cooled down to room temperature under N_2 gas, and the carbonized product was rinsed with 1 M HCl and deionized water to stable pH. After drying in an oven at 100 °C for 12 h, the solid was annealed in N_2 atmosphere at 900 °C for 3 h. All samples were stored under N_2 atmosphere before use.

2.2 Sample characterization

BET analysis of sample was performed on a Micromeritics ASAP 2020 using N_2 as adsorbate at -195.74 °C. Infrared spectra of biochar were collected on a Thermo Scientific FTIR 380 spectrometer at 400 - 4000 cm^{-1} with each sample mixed with KBr at 1:100 (w/w). Sample surface morphology was characterized by a JEOL JSM6700 scanning electron microscope equipped with an energy dispersive spectroscopy (EDS) detector and a high-resolution transmission electron microscope (HRTEM, JEOL JEM-2010). Elemental composition and chemical state on sample surface were detemined by XPS (ESCALAB 250 Xi, USA) analysis. Crystalline structure of biochar was characterized by a D/max-2500 X-ray diffractometer (XRD) with Cu-*ka* radiation (40 Kv, 250 Ma, k = 0.1789 nm) at a speed of 4°·min^{-1} and a scan 2θ range of 5^o - 80^o.

2.3 Electrochemical measurement

Electrochemical test was conducted on a CHI660A electrochemical workstation (CH instrument Co., China) with a three-electrode cell equipped with a gas-flow system. Counter and reference electrodes were a platinum sheet and a Hg/HgO (2 M KOH solution) electrode, respectively. Working electrode was a Φ3 mm glassy carbon electrode. In a typical electrochemical test, 5.0 mg biochar was added into 2 mL ethanol and 10 μL Nafion solution (1wt%, Alfa Aesar) and sonicated for 30 min to form a well-dispersed ink. Afterward, 10 μL dispersion was evenly spread on the glassy carbon electrode

and dried at room temperature for 2 h to develop a catalyst thin film. Commercial Pt/C catalyst was loaded onto the surface of electrode by the same method and used as reference in this experiment. After alkaline electrolyte (0.1 M KOH) was purged with high-purity N_2 or O_2 gas (99.99%) for 30 min to ensure gas saturated, cyclic voltammetry (CV) measurements were conducted over the potential range of -0.8 to +0.2 V (*vs* Hg/HgO) with a scan rate of 50 $mV \cdot s^{-1}$. Linear sweep voltammetry (LSV) measurements were conducted at a scan rate of 50 $mV \cdot s^{-1}$. The accelerated durability test (ADT) [28] was carried out in N_2-saturated 0.1 M KOH at -0.8 - +0.2 V with a scan rate of 50 $mV \cdot s^{-1}$.

3. RESULTS AND DISCUSSION

3.1 The morphology and composition of the catalyst

Scanning electron microscope (SEM) and transmission electron microscopy (TEM) were first used to analyze the physical morphology of the pyrolytic carbon materials. SEM image (Fig. 1a) shows BC-Zn contained a lot of curved fragments, which should be caused by the intense cleavage of biomass during pyrolysis owing to the catalytic role of $ZnCl_2$. High resolution SEM image (Fig. 1b) reveals the fragment of BC-Zn displayed a spongy-like structure, suggesting a large specific surface area of this sample. TEM (Figs. 1c and 1d) further confirms the presence of pore structure with varying sizes and open edge sites in BC-Zn. Published works reported that open edge sites and higher curvatures on carbon catalyst are favorable for ORR, because these structures may assist oxygen molecule to access conveniently and effectively to the electro-catalytic active sites [25-26].

Fig. 2 depicts the SEM (Figs. 2a and 2b) and TEM (Figs. 2c and 2d) images of BC-HP. From Fig. 2a, it can be seen that BC-HP comprised of many particles with different sizes. High-magnification SEM image (Fig. 2b) further reveals these particles had a rough surface with limited porous structures. TEM images (Figs. 2c and 2d) highlight the particle of BC-HP were not in the single-layer structure but had irregular open edges.

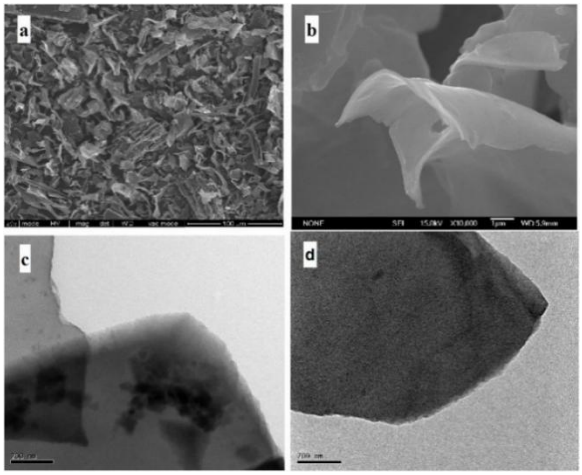

Figure 1. SEM (a and b) and TEM (c and d) images of BC-Zn

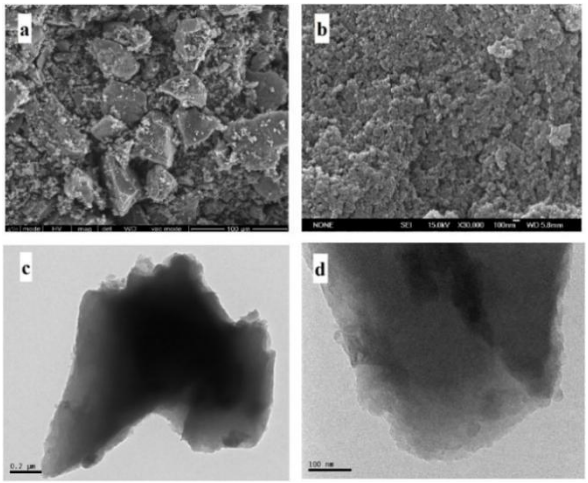

Figure 2. SEM (a and b) and TEM (c and d) images of BC-HP

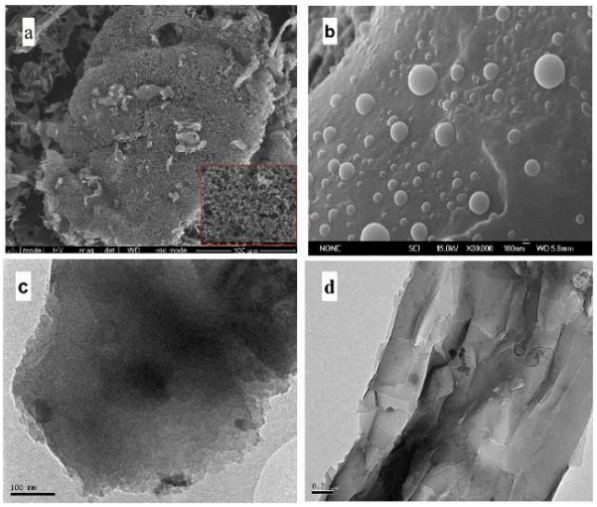

Figure 3. SEM (a and b) and TEM (c and d) images of BC-Na

Different from BC-HP and BC-Zn, BC-Na (Fig. 3a) was rich with micro/meso- pores, which were separated by regular interconnected channels (as shown in Fig. 3a insert). High-magnification SEM image (Fig. 3b) further reveals that the wall of the interconnected channel was rich with small bubbles (30-60 nm in diameter). TEM (Fig. 3c) indicates that BC-Na had an irregular, open edge and graphene-like structure. The microporous and mesoporous structure of BC-Na can also be confirmed by Fig. 3d.

The results of element analysis of samples are compiled in Table 1. It can be founded that nitrogen content in samples were 4.24%, 3.62% and 2.06% for BC-Zn, BC-HP and BC-Na, respectively (Table 1). Since no extra N was introduced in the preparation of biochar, it is considered that these N species come from the feedstock itself. Previous study reported N doping can significantly improve the oxygen reduction performance of catalyst [27]. Therefore, it is expected that these samples may have potentials in catalytic activity for oxygen reduction.

Table 1. Elemental analysis of BC-Zn, BC-HP and BC-Na

Samples	C (%)	N (%)	H (%)	O [a] (%)
BC-Zn	75.99	4.24	1.85	17.92
BC-HP	66.44	3.62	4.20	31.74
BC-Na	62.03	2.06	1.24	34.67

[a] assumed from the remainder of 100%, which didn't consider ash.

Figs. 4 and 5 show the DES analysis of BC-HP and BC-Na. It can also be found that BC-HP and BC-Na contained nitrogen, phosphorus and sulfur elements. The abundant P species in BC-HP is considered to derive from the phosphates deposit during the reaction of phosphoric acid and inherent alkaline-earth metals of biomass in pyrolysis. Moreover, N spots were detected in the EDS images of both BC-HP and BC-Na further confirmed that these nitrogen contents come exclusively from inherent N species of raw biomass.

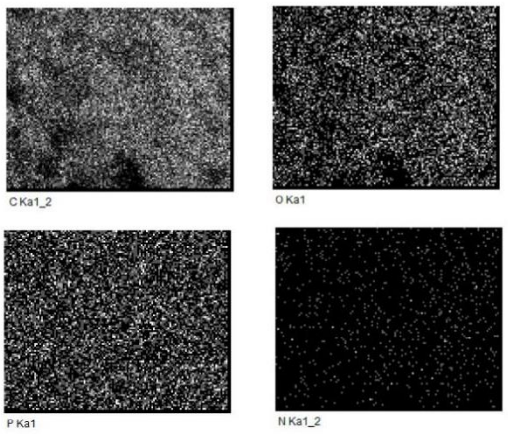

Figure 4. EDS images of BC-HP

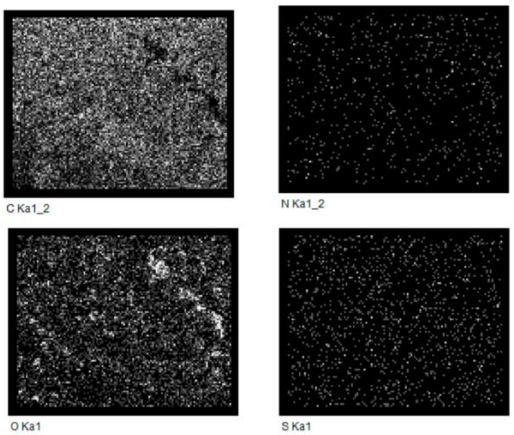

Figure 5. EDS images of BC-Na

Fig. 6a displays the X-ray diffraction (XRD) profile of three samples. As can be observed, all samples showed two obvious diffraction peaks at 2θ of 23.6° and 43.5°, with can be assigned to the (002) and (100) planes of a typical turbostratic carbon, respectively. This result demonstrates the graphitic carbon was developed in all samples after pyrolysis [28]. In addition, BC-Na exhibited four sharp peaks around 30.7°, 36.3°, 44.2° and 65.0°. According to XRD database, these peaks come from a high-degree graphitization structure of graphite, which is consistent with the result from SEM of BC-Na. Therefore, it can be inferred that a higher degree of structural alignment is more easily formed at high temperature pyrolysis.

N_2 adsorption-desorption isotherms were used to further analyze the porosity of BC-Na. As shown in Fig. 6b, the occurrence of the hysteresis loop at high pressure indicates the existence of mesopores in BC-Na, which is also in line with the SEM result. However, the sharp increase below a relative pressure of 0.1 is supposed to be caused by the micropores in sample. These results indicate BC-Na had both meso- and micro- pore structures. The pore size distribution calculated by the density functional theory (DFT) method indicates the prevalence of pores with a diameter of 2-4 nm in BC-Na. Surprisingly, the BET surface area, total pore volume and micropore volume of BC-Na reached 1337.27 $m^2 \cdot g^{-1}$, 0.847 $cm^3 \cdot g^{-1}$, and 0.507 $cm^3 \cdot g^{-1}$, respectively. These results indicate the etching effect of NaOH during the high temperature pyrolysis made the raw biomass transform into a porous nanomaterial. High porosity with mesoporous structure was also considered to be beneficial for ORR activity due to the increased surface area and abundance in catalytic sites [29].

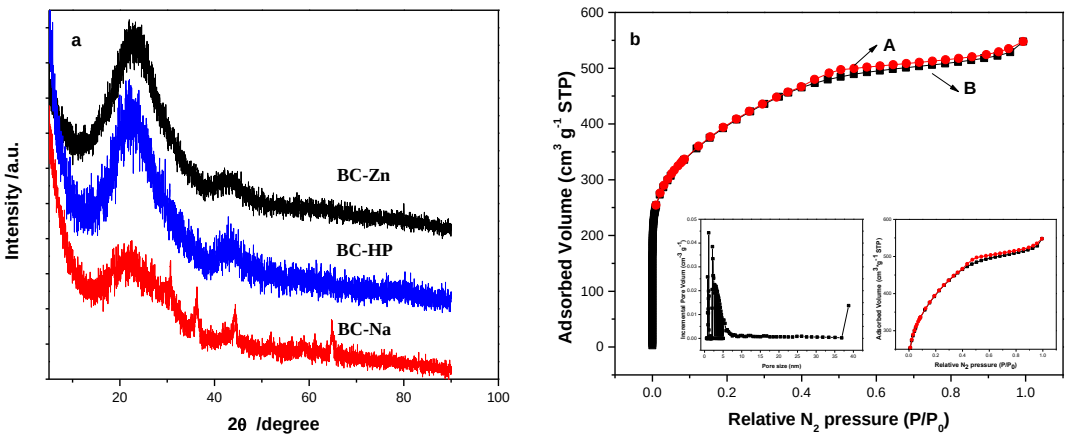

Figure 6. (a) XRD patterns of BC-HP, BC-Zn and BC-Na and (b) Nitrogen adsorption (A)-desorption (B) isotherms at 77 K and DFT pore-size distribution (inset) of BC-Na

The XPS scan, high-resolution N1s spectra and high-resolution S2p were used to further investigate the nitrogen and sulfur configuration in BC-Na. As shown in Fig. 7a, BC-Na displays a typical C1s peak at 284 eV, N1s peak at 400 eV and an O1s peak at 532 eV, which proved that this sample is indeed a nitrogen self-doping carbon material. The ORR activity of N-doped carbon catalyst depends highly on nitrogen configuration. To analyze the nitrogen bond configuration, the N1s peak

(Fig. 7b) was deconvoluted into four nitrogen groups, pyridinic-N (398.2 ± 0.3 eV), pyrrolic-N (400.5 ±0.3 eV) and quaternary or graphitic-N (401.1 ± 0.3 eV), respectively [30-32]. As can be observed, BC-Na was rich with pyridinic-N and pyrrolic-N, which have planar structure and are active to ORR [33]. The binding energy of XPS-S2p was also used to analyze sulfur doping. As shown in Fig. 7c, the former two peaks are S2p 3/2 (162.9±0.2 eV) and S2p 1/2 (164.9±0.2 eV), which were assigned as the vibration of spin-orbit coupling of thiophene-S [34,35]. According to above results, both N and S was doped into the carbon skeleton BC-Na.

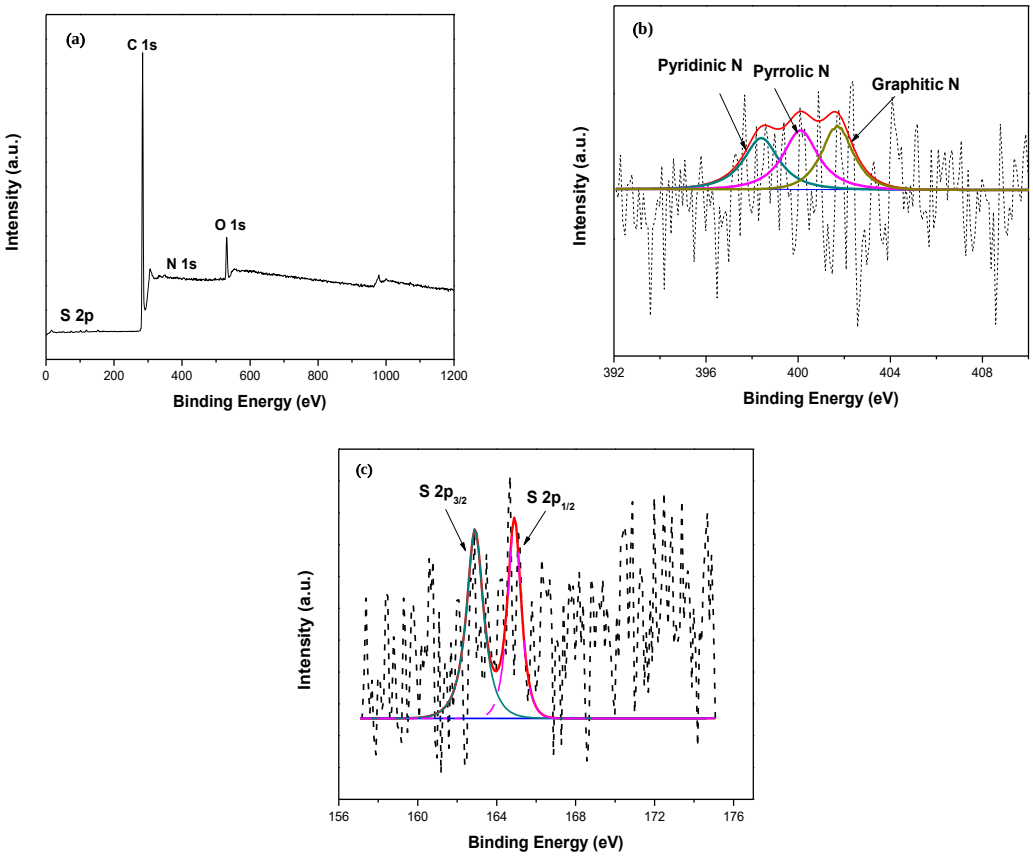

Figure 7. XPS spectra of surface chemical composition (a) and high-resolution N1s spectra of (b), high-resolution S2p (c) of BC-Na

3.2 Electrocatalytical activities

The electro-catalytic properties of three catalysts were first investigated under alkaline (0.1 M KOH) condition at room temperature by cyclic voltammetry (CV) in O_2-saturated solution and N_2-saturated solution from -0.8 to +0.2 V (*vs* Hg/HgO), respectively.

The results in the alkaline media (0.1 M KOH) are shown in Fig. 8. The CV curves display quasi-rectangular voltammograms in N_2-saturated 0.1 M KOH solution for all samples. After oxygen was introduced into electrolyte, a well-defined oxygen reduction cathodic peak can be observed from Figs. 8a-d, demonstrating these samples were active to ORR. In paricular, BC-Zn exhibites a more negative shift of -0.42 V of reduction peak potential relative to BC-HP (-0.31 V) and BC-Na (-0.31 V). Zhu et al

[36] used phosphorus doped porous carbon as ORR catalyst and found that the oxygen reduction potential was -0.285 V, which is close to -0.31 V from BC-HP and BC-Na, but the current density of phosphorus doped carbon was higher than that in this paper, which may be caused by the difference of raw material and preparation condition. By using $ZnCl_2$ as an activator, Liu et al [37] reported that biochar can achieve an oxygen reduction potential of 0.81 V, but the current density was 1 $mA \cdot cm^{-2}$, which is lower than BC-Zn. Meanwhile, the net peak current density of BC-Na reached about 2.63 $mA \cdot cm^{-2}$ by subtracting the background current from the current density. This value is significantly higher than that of BC-HP (2.45 $mA \cdot cm^{-2}$) and BC-Zn (2.39 $mA \cdot cm^{-2}$). Table 2 compared the electrocatalytic activities of the biochar with some previous studies. As can be obesrved, the catalysts obtianed in this expriment, in particular BC-Na, show much higher current density than other samples[38,39].

Linear sweep voltammetry (LSV) in O_2-staturated 0.1 M KOH solution at room temperature was also tested, and the results are compiled in Fig. 8e. It clearly demonstrats the difference in ORR activity of these samples. BC-Na exhibited a more negative ORR onset potential (E=-0.21 V) than Pt/C (E=0.09V), while its current density (j =-5.72 $mA \cdot cm^{-2}$) is higher than Pt/C (j = -3.25 $mA \cdot cm^{-2}$). Wu et al [40] compared the ORR performance of P-C with Pt/C, and found that both the initial potential and current density of P-C were lower than Pt/C. In this study, however, BC-Na presneted a much higher current density in contrast to Pt/C, which highlights the potential of BC-Zn as a catalyst.

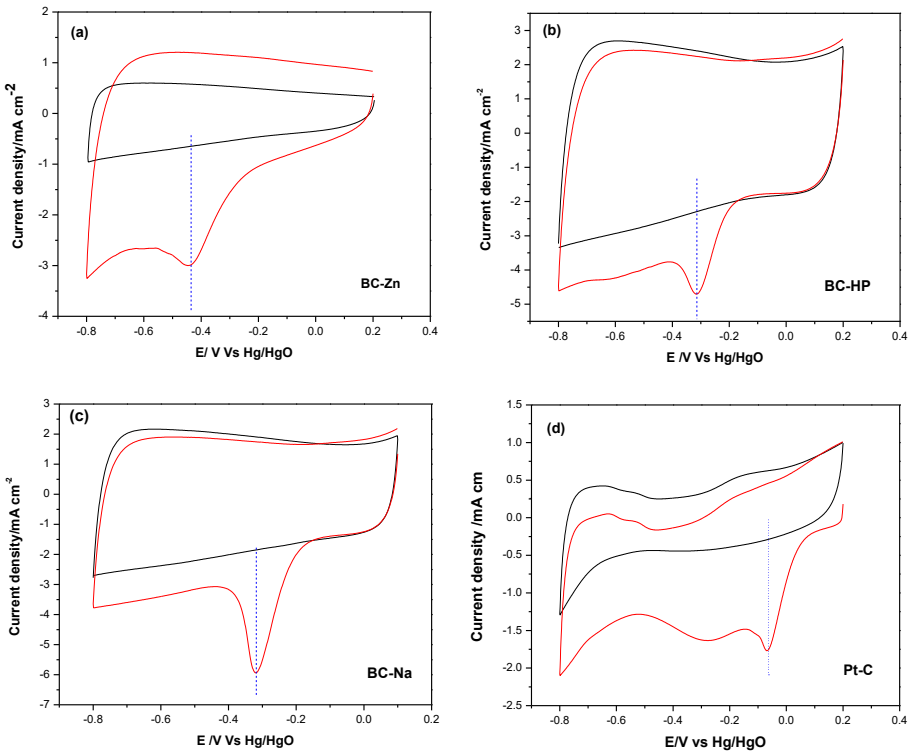

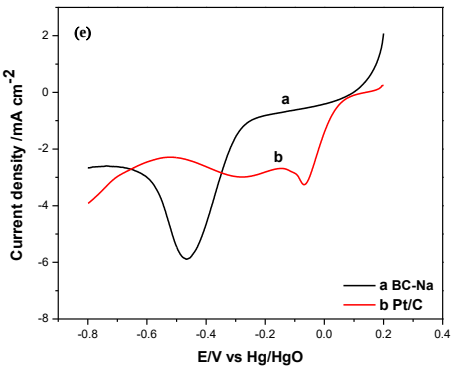

Figure 8. (a~d) Cyclic voltammograms of BC-Zn, BC-HP, BC-Na and 20% Pt/C in N_2 (black) and O_2-saturated (red) 0.1 M KOH, (e) Linear sweep voltammetry (LSV) measurement of BC-Na and 20% Pt/C

Based upon above results, BC-Na demonstrated the better ORR electro-catalytic activity than BC-Zn and BC-HP. In this study, BC-Na was prepared by first pyrolyzing the biomass at 250 °C to make the cellulose in feedstock cracked to develop internal channel. After that, NaOH powder was introduced to react with biomass under mild condition (600 °C) to expand these channels. Finally, high temperature annealing under 900 °C led to the formation of an orderly structure of graphite carbon in BC-Na. Both the large specific surface area and orderly graphite structure [41] contribute the better ORR performance. This may be the reason of high ORR performance of BC-Na.

Table 2. The eletrocatalytic properties of ORR catalysts prepared by difference methods

Sample	Limiting current density ($mA \cdot cm^{-2}$)	Onset potential (V)	Reference
MC	-	-0.203	
MC-IP	-	-0.188	[36]
MC-OP	-	-0.174	
WHC-600	0.21	+0.84	
WHC-700	1.04	+0.98	[37]
WHC-800	0.59	+0.91	
PN-rGO	0.96	-0.21	[38]
NPC@AC-0.7	1.07	+0.15	[39]
BC-HP	2.45	-0.31	
BC-Zn	2.39	-0.42	This work
BC-Na	2.63	-0.31	

4. CONCLUSIONS

In this work, a facile and mild approach was proposed to fabricate porous nitrogen doped catalyst with a high surface area (up to 1337.27 $m^2 \cdot g^{-1}$) from corn stalks, a natural, abundantly available, and

recyclable biomass. Benefiting from the favorable structure and chemical composition, the ORR electro-catalytic activity of BC-Na is higher than BC-Zn and BC-HP. The ORR performance of BC-Na is comparable to 20% commercial Pt/C catalysts with an oxygen reduction current density up to 5.72 $mA \cdot cm^{-2}$.

ACKNOWLEDGEMENTS
This work was financially supported by National Nature science Foundation of china (NSFC) (No. 41877123).

References

1. B.C.H. Steele, A. Heinzel, *Nature*, 414(2001)345.
2. R. Cao, R. Thapa, H. Kim, X. Xu, M.G. Kim, Q. Li, N. Park, M.L.J. Cho, *Nat. Commun*., 4(2013)2076.
3. C. Wang, N.M. Markovic, V.R. Stamenkovic, *ACS Catal.*, 2(2012)891.
4. J. Greeley, I.E.L. Stephens, A.S. Bondarenko, T.P. Johansson, H.A. Hansen, T.F. Jaramillo, I.C.J. Rossmeisl, J.K. Nørskov, *Nat. Chem*., 1(2009)552.
5. V. Dinoto, E. Negro, *Fuel Cells*, 10(2010)234.
6. G. Wu, P. Zelenay, *Chem. Res.,* 46(2013)1878.
7. K. Gong, F. Du, Z. Xia, M. Durstock, L. Dai, *Science*, 323(2009) 760.
8. Y. Shao, J. Wang, H. Wu, J. Liu, I. A. Aksay, Y. Lin, *J. Mater. Chem*., 20(2010)7491.
9. D. Geng, Y. Chen, Y. Chen, Y. Li, R. Li, X. Sun, S. Knights, *Energy. Environ. Sci*., 4(2011) 760.
10. Y. Li, W. Zhou, H. Wang, L. Xie, Y. Liang, F. Wei, H. Dai, *Nature Nanotech.,* 7(2012) 394.
11. P. Chen, T.Y. Xiao, Y.H. Qian, S.S. Li, S.H. Yu, *Adv. Mater*., 25(2013)3192.
12. W. Yang, T.P. Fellinger, M. Antonietti, *J. Am. Chem. Soc*., 133(2010)206.
13. S. Chen, J. Bi, Y. Zhao, L. Yang, C. Zhang, Y. Ma, Z. Hu, *Adv. Mater*., 24(2012)5593.
14. H. Liu , X. Wang , W. Cui , Y. Dou , D. Zhao , Y. Xia , *J. Mater. Chem.*, 20(2010)4223.
15. Z. Li, Z. Xu, X. Tan, H. Wang, C.M.B. Holt, T. Stephenson, B.C. Olsen, D. Mitlin, *Energy Environ. Sci*, 6(2013)871.
16. F. Pan, Z. Cao, Q. Zhao, H. Liang, J. Zhang, *J. Power Sources*, 272(2014)8.
17. Z. Li, L. Zhang, B.S. Amirkhiz, X. Tan, Z. Xu, H. Wang, B.C. Olsen, C.M.B. Holt, *Adv. Energy Mater.,* 2(2012)431.
18. H. Yang, Z. Tang, K. Wang, W. Wu, Y. Chen, Z. Ding, S. Chen, *J. Colloid. Interface Sci*., 528(2018)18.
19. X. Li, B.Y. Guan, S. Gao, *Energy. Environ. Sci*., 12(2019).
20. G. Wu, P. Zelenay, *Science*, 332(2011)443.
21. Z. Mo, S. Liao, Y. Zheng, Z. Fu, *Carbon,* 50(2012)2620.
22. L. Mu, R. Wang, C. Tang, *Biomass Convers Bior*., 9(2019)401.
23. H. Zhou, J. Zhang, I.S Amiinu., C. Zhang, X. Liu, W. Tu, S. Mu, *Phys. Chem. Chem. Phys*., 18(2016)10392.
24. W. Cao, B. Wang, Y. Xia, W. Zhou, J. Zhang, R. Wen, Y. Jia, Q. Liu, *Int. J. Electrochem. Sci*., 14(2019)250.
25. B. Frank, M.E. Schuster, R. Schlçgl, D. S. Su, *Angew. Chem. Int. Ed*., 52(2013)2673.
26. C. Hu, Y. Xiao, Y. Zhao, N. Chen, Z. Zhang, M. Cao, L. Qu, *Nanoscale*, 5(2013)2726.
27. X. Bao, X. Nie, D .V. Deak. *Top. Catal.*, 56(2013)1623.
28. J. Wu, Z. Yang, X. Li, Q. Sun, C. Jin, P. Strasser, R. Yang, *J. Mater. Chem. A,* 1(2013)9889.
29. F. Liu, H. Peng, X. Qiao, Z. Fu, P. Huang, S. Liao, *Int. J. Hydrogen Energy*, 39(2014)10128.
30. J. Yu, C. Wang, W. Yuan, Y. Shen, A. Xie, *Chem.-- Eur. J.*, 25(2019), 2877.

31. M. Shao, Q. Chang, J.P. Dodelet, R. Chenitz, *Chem. Rev*., 116(2016) 3594.
32. S. Yang, X. Feng, X. Wang, K.M. Llen, *Angew. Chem. Int. Ed.*, 50(2011)5339.
33. K. Han, J. Shen, S. Hao, H. Ye, C. Wolverton, M.C. Kung, H.H. Kung, *ChemSusChem*. 7(2014)2545.
34. Z. Guo, G. Ren, C. Jiang, X. Lu, Y. Zhu, L. Jiang, L. Dai, *Sci. Rep.,* 5(2015)17064.
35. S. K. Kim, Y. Qiu, Y. J. Zhang, R. Hurt, A. Peterson, *Appl. Catal., B* 235(2018)36.
36. Y.P. Zhu, Y. Liu, Y.P. Liu, *ChemCatChem,* 7(2015)2903.
37. X. Liu, Y. Zhou, W. Zhou, *Nanoscale,* 7(2015).
38. X.Qiao , S.Liao , C.You . *Catalysts*,5(2015)981.
39. K.Lv , H.Zhang ,S. Chen . *RSC adv*., 8(2018)848.
40. J. Wu, Z.Yang, X. Li, Q. Sun, C. Jin, *J. Mater. Chem. A*, 1(2013).
41. L.L. Zhang, X. Zhao, H. Ji, *Energy Environ. Sci.*, 5(2012)9618.